

## Molecular Dynamics Simulation For Barium Zirconate Proton Conducting Oxide Energy Materials: A Mini Review

M. Khalid Hossain

Interdisciplinary Graduate School of Engineering Science, Kyushu University

M. Ishak Khan

University of Pennsylvania

T. Sarkar Akash

Bangladesh University of Engineering and Technology

Hashizume, Kenichi

Interdisciplinary Graduate School of Engineering Science, Kyushu University

<https://doi.org/10.5109/4738550>

---

出版情報 : Proceedings of International Exchange and Innovation Conference on Engineering & Sciences (IEICES). 7, pp.1-6, 2021-10-21. Interdisciplinary Graduate School of Engineering Sciences, Kyushu University

バージョン :

権利関係 :



# Molecular Dynamics Simulation For Barium Zirconate Proton Conducting Oxide Energy Materials: A Mini Review

M. Khalid Hossain<sup>1,2\*</sup>, M. Ishak Khan<sup>3</sup>, T. Sarkar Akash<sup>4</sup>, Kenichi Hashizume<sup>1</sup>

<sup>1</sup>Interdisciplinary Graduate School of Engineering Science, Kyushu University, Kasuga, Fukuoka 816-8580, Japan,

<sup>2</sup>Atomic Energy Research Establishment, Bangladesh Atomic Energy Commission, Dhaka 1349, Bangladesh,

<sup>3</sup>University of Pennsylvania, Philadelphia, PA 19104, USA,

<sup>4</sup>Bangladesh University of Engineering and Technology, Dhaka-1000, Bangladesh.

\*Corresponding author email: khalid.baec@gmail.com, khalid@kyudai.jp

**Abstract:** Barium zirconate ( $\text{BaZrO}_3$  or BZO) is a proton conducting perovskite material with a wide range of uses, including protonic ceramic fuel cells, electrolyzers, and catalytic membrane reactors that operate at temperatures ranging from 873 to 1073 K. A large number of experimental repertoires have established desired manipulations of structural and thermodynamic parameters such as grain size, sintering, etc. However, atomistic simulation studies such as molecular dynamics (MD) and density functional theory (DFT) have complemented the experimental findings and provided critical insight into proton conducting mechanism, electron hopping mechanism, and so on. Therefore, to comprehend proton conducting mechanism in atomic resolution, considering the MD works is necessary. It will not only pave the pathway for further improvement of proton conducting maneuvers but also facilitate regulating critical parameters at nanoscale. In this regard, this review work briefly reports the insights obtained from MD studies on BZO.

**Keywords:** Molecular dynamics simulation, barium zirconate, proton conducting oxide, energy materials.

## 1. INTRODUCTION

Perovskite materials are relevant in hydrogen pumps [6], hydrogen sensors [1], hydrogen isotope separator, tritium monitoring, tritium purification [2–7], and recovery [3,8–12] in nuclear fusion reactors sectors. Among them, one of the most widely explored materials is  $\text{BaZrO}_3$  due to its diversified application and doping characteristics [13–19]. Over the last four decades, their implementation has been recognized through different experimental synthesis techniques, and their utilization has been realized due to their desired structural and thermodynamic behavior in multifarious applications. However, in many cases, experimental techniques are useful at macroscale, while understanding the mechanism of specific functionality requires insight at an atomistic level. In this regard, MD simulation studies are highly relevant due to their capability of capturing structural, thermodynamic, and electronic configuration and exchange behavior. Therefore, this brief study reports the utility of MD simulation with regard to  $\text{BaZrO}_3$ .

## 2. APPLICATION OF PROTON CONDUCTORS IN RENEWABLE ENERGY FIELD

Renewable energy can be introduced in a large scale and as a long-term stable main power source that may play a major role in the world's energy supply. Renewable energy has a low energy density and needs to be concentrated. Therefore, attention is being paid to electrolysis (electrolysis) technology of water and water vapor, which uses renewable energy as primary energy and converts it into hydrogen, which is secondary energy. Water electrolysis is classified according to the operating temperature, the type of electrolyte, and methods such as alkaline water electrolysis and solid polymer type water electrolysis have already been put into practical use. However, when water electrolysis is compared with the conventional hydrogen production method, it is known to be inferior in terms of cost. On the other hand, steam electrolysis is characterized by operating at high temperature using a solid electrolyte, and it may improve the energy efficiency of electrolysis, which is thought to lead to a reduction in the cost of hydrogen production.

Normally, yttria-stabilized zirconia, which is an oxide ion conductive electrolyte, is used as a solid electrolyte, but the application of proton conductive electrolytes is being studied from the viewpoint of electrical conductivity. Fig. 1 shows the schematic diagram of steam electrolysis using an oxide ion conductor and a proton conductor. When an oxide ion conductor is used as an electrolyte (Fig. 1(a)), water vapor is introduced to the cathode side, water is electrochemically separated into hydrogen and oxide ions, and the oxide ions are oxidized on the cathode side to generate oxygen. On the other hand, in case of a proton conductor (Fig. 1(b)), water vapor is introduced not on the cathode side but the anode side and hydrogen are generated on the cathode side in a form separated from water vapor. When steam electrolysis is considered as a hydrogen production

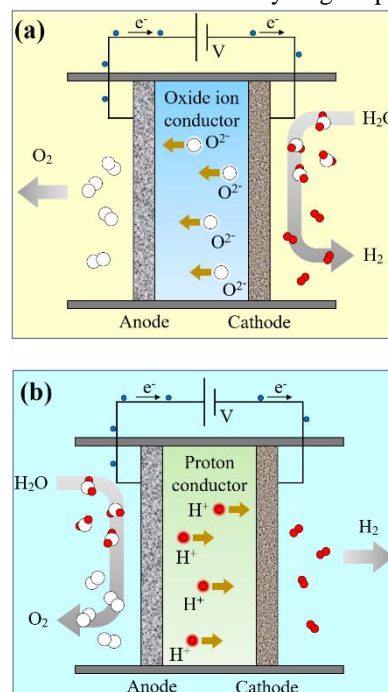


Fig. 1. Schematic diagram of steam electrolysis using (a) oxide ion conductor, and (b) proton conductor.

method, it is not necessary to separate hydrogen from high-concentration steam, which is considered to be one of the advantages of selecting a proton conductor as a solid electrolyte.

### 3. OVERVIEW OF MD SIMULATION

The conspicuous contribution of MD simulation to proton conductor studies can be grossly divided as below in terms of understanding specific attributes:

- Proton diffusion across grain boundary,
- Proton mobility,
- Doping mechanism,
- Transportation of oxygen ion,
- Manipulation of structural and thermodynamic properties.

In the following sub-sections, these aspects are discussed without incorporating redundancy.

#### 3.1 Review on MD simulation of BZO

In 2008, Van Duin *et al.* [20] developed a reactive force field (Reaxff) for bulk phase Y-doped BaZrO<sub>3</sub> to study proton diffusion across the grain boundary using molecular dynamics (MD) simulations (Fig. 2). They concluded that grain boundaries increase the average distances between oxygens that are in separate interfaces which facilitate the increase in proton hopping barriers. This increase in proton hopping barriers consequently results in reduction of proton diffusions. Their findings using reaxff MD simulation are in good agreement with experimental results which validates the force field to use in atomistic modelling and analysis of bulk BYZ phase [20]. This study also paved the way for a decade of simulation-based studies using this force field.

Cammarata *et al.* [21] studied structural changes and proton mobility for undoped, singly and doubly Y-doped BaZrO<sub>3</sub> with varying temperature (100 to 1200 K) using reaxff MD simulation. First of all, the relation of cell parameter  $a$  is found to be linear and positive with temperature. The extrapolated value of  $a$  at 77 K, 4.22 Å and coefficient of thermal expansion  $2.42 \times 10^{-5}/\text{K}$  were very close to experimental findings. Radial distribution function of O-O couple had different means for different temperature and Y-doping content which indicate that the oxygen subnetwork is temperature and doped yttrium content dependent. Protonation also caused softening in the matrix and as a result the force becomes constant between different couples. The calculated activation energy for undoped, singly and doubly doped structures were 0.32, 0.40 and 0.47 eV which were in good agreement with corresponding experimental values of 0.46, 0.43 and 0.43 eV respectively [22]. For oxygens in singly doped structure, three stable sites were found having activation energies of 0.05, 0.23, and 0.28 eV respectively, whereas for doubly doped structures these energies were 0.17, 0.45, and 0.31 eV respectively. Yttrium clustering was also evident in doubly doped structure that enabled two of the three stable oxygen sites in structure to be multilevel protonic traps resulting in a delayed protonic diffusion.

Li *et al.* [23] studied fast oxygen transport in Y-doped BaZrO<sub>3</sub> using reactive molecular dynamics simulation (Fig. 3). The effect of yttrium concentration and dislocations on oxygen ion conduction, migration mechanism, and structural properties was thoroughly investigated. For bulk structure, the diffusion coefficient ( $D_0$ ) increased when yttrium mol % concentration increased from 10 to 20 and then gradually decreased

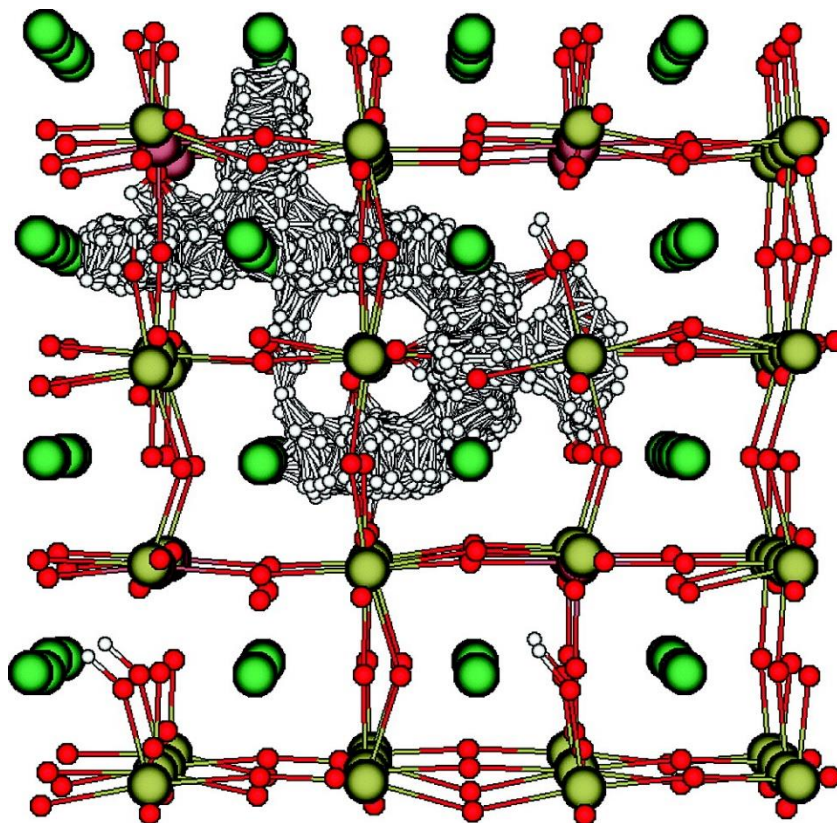


Fig. 2. ReaxFF MD simulation on Y-doped BaZrO<sub>3</sub> at T =1000 K, t = 1.5 ns shows the trajectory of one hydrogen atom (represented by tiny white spheres) [20].



when yttrium mol % was increased to 36. In the case of structures with dislocations,  $D_0$  increased with yttrium mol % up to 30 and then decreased except for 25 mol %

yttrium. These indicate that 20 and 30 mol % yttrium yielded the highest value of  $D_0$  for bulk and line dislocated structures respectively.  $D_0$  ranges from  $6.22 \times$

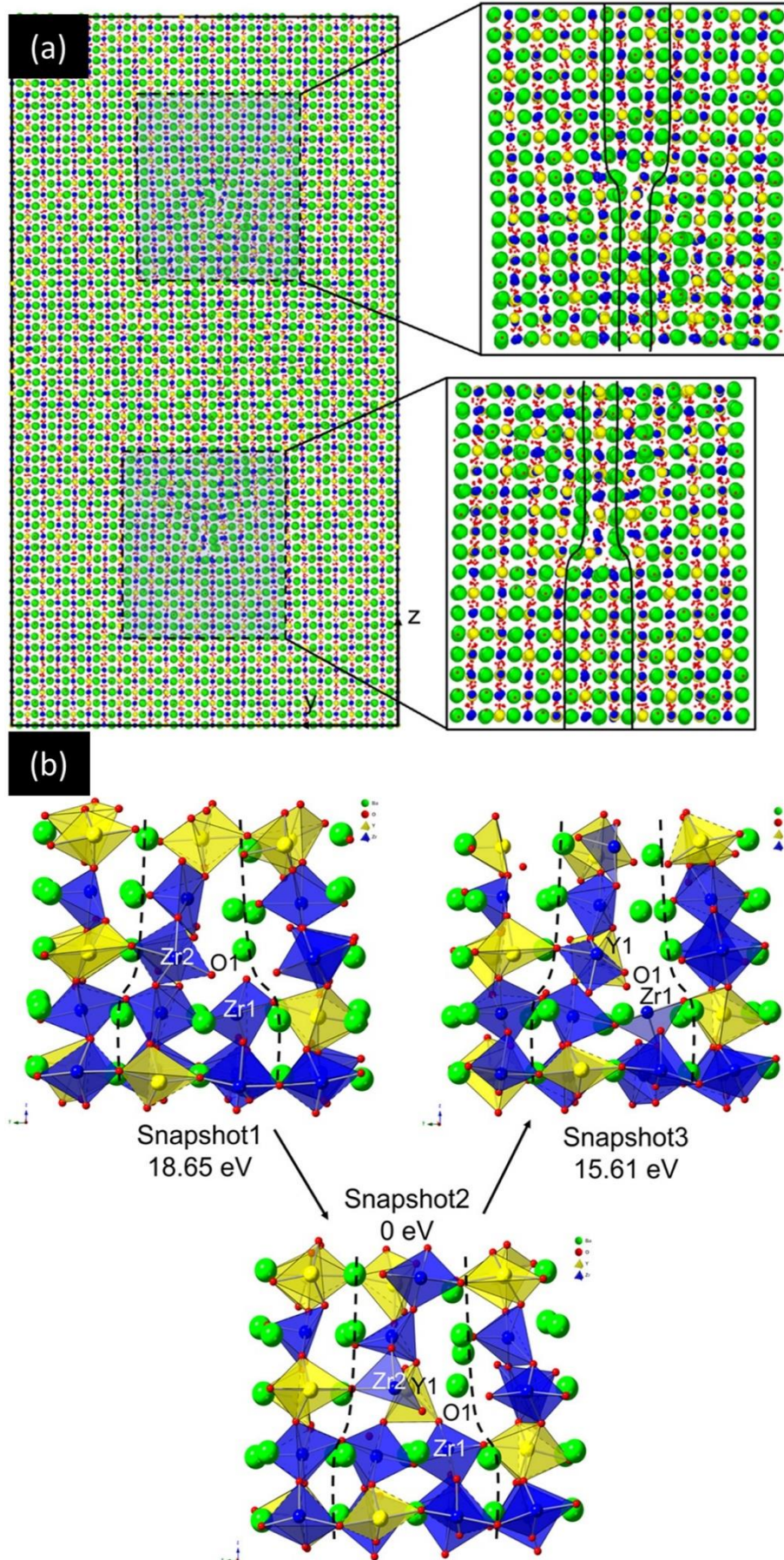


Fig. 3. (a) In edge dislocation, the profile of a double-bottle diffusion channel for 30% Yttrium-doped barium zirconate (Y30), (b) mechanism of  $O^{2-}$  diffusion in Y30 around the dislocation core has been identified [23].

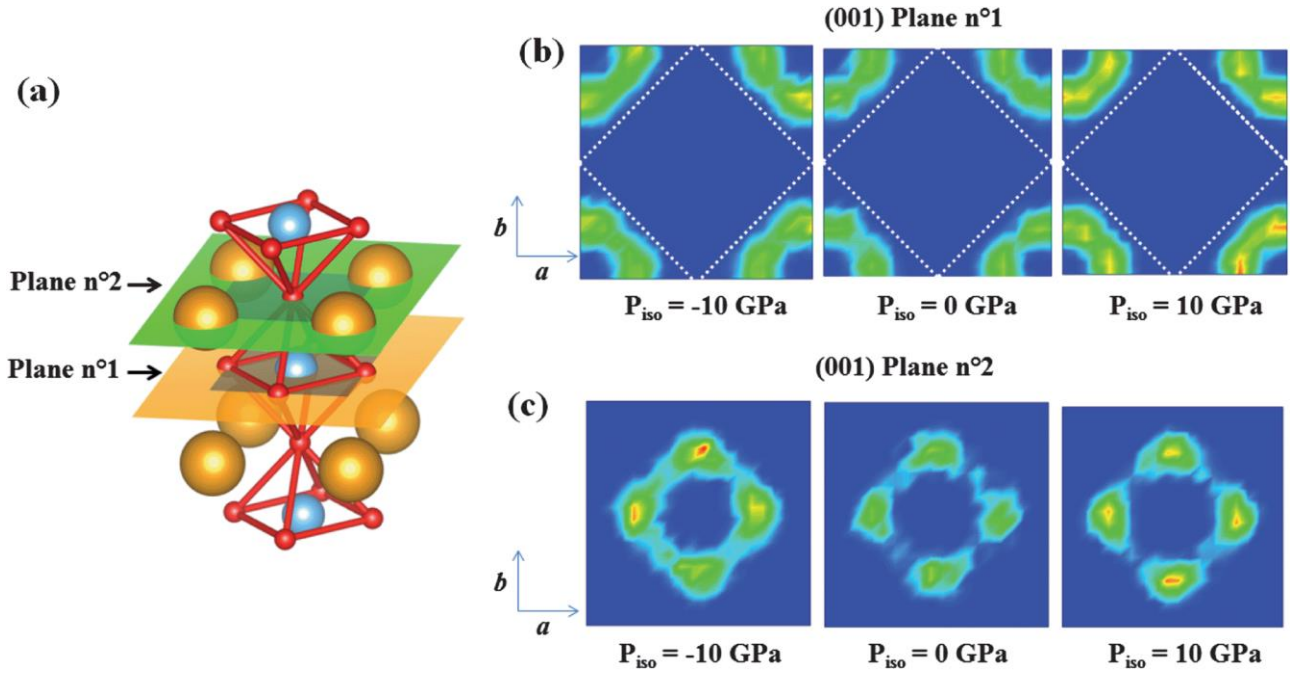


Fig. 4. Proton density maps for 1% Y-doping on the cation B-site determined at  $T = 2000$  K at isotropic pressures of 10, 0, and 10 GPa. (a) The two planes in which the proton density is indicated are represented schematically in the perovskite structure. The spheres indicate atomic locations, with gold, blue, and red representing Ba, Zr, and O, respectively. (b) Maps of proton density for plane n°1 with oxygen–oxygen bonds. (c) Density maps of protons in plane n°2 with oxygen and barium atoms (note: only the density of protons is displayed). The density is color coded here from blue (zero density) to red (high density) (high density) [31].

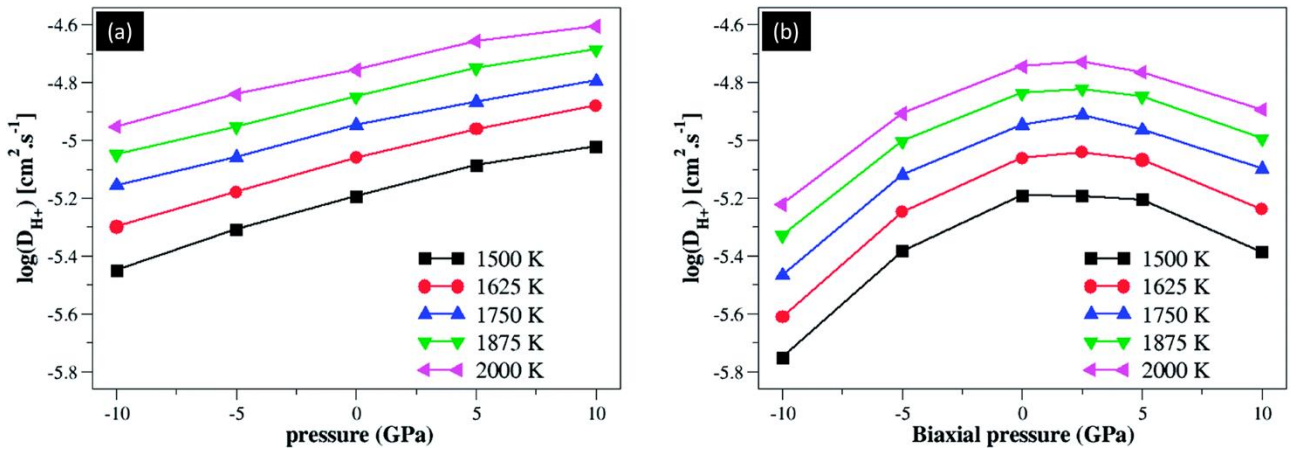


Fig. 5. (a) For barium zirconate with 12.5 percent Y doping, proton diffusion coefficients were calculated as a function of isotropic pressure at various temperatures. (b) For barium zirconate with 12.5 percent Y doping, proton diffusion coefficients were calculated as a function of biaxial pressure at various temperatures [31].

$10^{-7}$  to  $8.19 \times 10^{-7} \text{ cm}^2\text{s}^{-1}$  and  $2.90 \times 10^{-7}$  to  $8.85 \times 10^{-7} \text{ cm}^2\text{s}^{-1}$  for Bulk structures and structures with dislocations respectively. These values of  $D_0$  are close to the experimentally achieved value of  $6.6 \times 10^{-8} \text{ cm}^2\text{s}^{-1}$  at 1073 K [24]. The relation between  $D_0$  and temperature was found to be linear and positive. Below 1173.15 K, the  $D_0$  of dislocated 30 mol % yttrium containing structure is higher than 20 mol % yttrium containing bulk structure which was previously confirmed for  $\text{SrTiO}_3$  at 1200 K. Below 1173.15 K, dislocation facilitates forming of a double bottle-like channel that accelerates oxygen ion diffusion by reorienting oxygen polyhedron. The ionic conductivity of oxygen ions, beyond 1073.15 K increased with mol % yttrium content up to 20 and then decreased gradually, whereas, below 1073.15 K, the

highest ion conductivity was at 10 mol % yttrium content and declining afterward. At critical temperature 1073.15 K, the highest ionic conductivity was found for 15 mol % yttrium.

Kurosaki *et al.* [25] calculated the coefficient of thermal expansion using molecular dynamics simulation with a semi-empirical two-body potential and found it to be  $7.91 \times 10^{-6} \text{ K}^{-1}$  which was close to the theoretical results [26]. They also figured that the thermal conductivity decreases with increasing temperature also supporting the experimental trend [26].

Goh *et al.* [27] used mixed potential consisting coulombic interaction, c, short-range repulsion, and morse type covalent interaction to enable non-equilibrium molecular dynamics simulation of  $\text{BaZrO}_3$ .



Their calculated cell parameter  $4.292 \text{ \AA}$  and coefficient of thermal expansion  $8.16 \times 10^{-6} \text{ K}^{-1}$  are very close to the experimentally obtained value of  $4.1928 \text{ \AA}$  [28] and  $7.13 \times 10^{-6} \text{ K}^{-1}$  [29]. They calculated isothermal compressibility, heat capacity, thermal conductivity were  $7.34 \times 10^{-12} \text{ Pa}^{-1}$ ,  $110.8 \text{ J mol}^{-1} \text{ K}^{-1}$ , and  $4.26 \text{ W m}^{-1} \text{ K}^{-1}$  at room temperature respectively which are also in close agreement with experimental findings [26,29,30].

Ottocian *et al.* [31] used reactive molecular dynamics simulation to study the effect of isotropic and biaxial strain on proton conduction in yttrium doped  $\text{BaZrO}_3$  at different temperatures (1500 to 2000 K) (Figs. 4 and 5). In general, the proton diffusion coefficient  $D_0$  increased with temperatures. For low concentration of yttrium doping (1%) and isotropic strain,  $D_0$  increased from  $1.19 \times 10^{-3} \text{ cm}^2 \text{ s}^{-1}$  to  $1.27 \times 10^{-3} \text{ cm}^2 \text{ s}^{-1}$  and activation energy decreased from 0.51 eV to 0.39 eV with pressure changing from -10 to 10 GPa. An increase in isotropic pressure reduces the O-O distances and thus increasing proton diffusion coefficient. But in the case of biaxial pressure, at first,  $D_0$  increases by  $\sim 2$  times up to 2.5 GPa and then gradually decreases, and activation energy decreased from 0.59 eV to 0.42 eV and then again increasing to 0.52 eV. This is because an increase in pressure results in the localization of the protons strongly away from the B-cation. At excessive-high biaxial pressure, the cause of reduction if  $D_0$  results from both increases in O-O distance and proton localization. Their study exhibits the limitation of strain engineering in  $\text{BaZrO}_3$ .

Kitamura *et al.* [32] studied the effect of zinc and yttrium doping in  $\text{BaZrO}_3$  using DFT-based molecular dynamics simulation. Their study demonstrated that without doping the value of  $D_0$  was  $1.3 \times 10^{-5} \text{ cm}^2 \text{ s}^{-1}$  which is close to experimental results [26]. They showed that Zn- and Y-doping caused protons to be localized more around Zn than Y which consequently increased proton trapping and ultimately reducing the coefficient of proton diffusion to  $3.9 \times 10^{-5} \text{ cm}^2 \text{ s}^{-1}$ .

### 3.2 Prospects and challenges of MD simulation for BZO

From the previous section, it is evident that FP, DFT, and MD simulation studies have provided appropriate validations for experimental works on  $\text{BaZrO}_3$  in terms of explaining the proton conduction mechanism, proton hopping, and ion exchange mechanism, thermal and structural attributes, and so on. These contributions will certainly play an instrumental role to explore further criteria of implementation of this perovskite material, especially from the doping perspective, as atomistic simulation captures mechanical and structural behavior at atomic resolution. Although the utilization of MD is mostly found for  $\text{BaZrO}_3$  due to its vast application among other perovskites, such validation-focused maneuvers can certainly be expanded for other perovskite and rare earth materials, especially to explore their interaction with target materials with required properties. However, the main challenge from the simulation front is the lack of appropriate force fields for each scenario, which is one of the points of interest of computational material scientists. As the theoretical groundwork of MD simulation mostly depends on empirical characterization, a fast-paced experimental

advancement in the next few years will come at aid to address this particular challenge.

## 4. CONCLUSIONS

The findings of the study are summarized as below:

- MD simulation studies on BZO facilitated explaining critical research questions involving proton diffusion across grain boundary, proton mobility in doped conformation, ion transport, and non-bonded interactions.
- For the validation of the significant number of experimental works going on focusing on  $\text{BaZrO}_3$ , MD simulation holds a prospective ground, provided that the limitations of the force field are addressed in a timely manner.

## 5. REFERENCES

- [1] L. Dai, L. Wang, G. Shao, Y. Li, A novel amperometric hydrogen sensor based on nano-structured ZnO sensing electrode and  $\text{CaZr}_{0.9}\text{In}_{0.1}\text{O}_{3-\delta}$  electrolyte, *Sensors Actuators B Chem.* 173 (2012) 85–92.
- [2] Y. Kawamura, S. Konishi, M. Nishi, T. Kakuta, Transport Properties of Hydrogen Isotope Gas Mixture Through Ceramic Protonic Conductor, *Fusion Sci. Technol.* 41 (2002) 1035–1039.
- [3] Y. Kawamura, S. Konishi, M. Nishi, Extraction of Hydrogen from Water Vapor by Hydrogen Pump Using Ceramic Protonic Conductor, *Fusion Sci. Technol.* 45 (2004) 33–40.
- [4] A. Ciampichetti, F.S. Nitti, A. Aiello, I. Ricapito, K. Liger, D. Demange, L. Sedano, C. Moreno, M. Succi, Conceptual design of Tritium Extraction System for the European HCPB Test Blanket Module, *Fusion Eng. Des.* 87 (2012) 620–624.
- [5] H. Iwahara, Study on proton conductive solid electrolyte-recent trends, *Electrochemistry.* 69 (2001) 788–793.
- [6] O. Antoine, C. Hatchwell, G.C. Mather, A.J. McEvoy, Structure and Conductivity of a Yb-Doped  $\text{SrCeO}_3\text{-BaZrO}_3$  Solid Solution, *ECS Proc. Vol.* 2003–07 (2003) 379–387.
- [7] Y. Kawamura, T. Yamanishi, Tritium recovery from blanket sweep gas via ceramic proton conductor membrane, *Fusion Eng. Des.* 86 (2011) 2160–2163.
- [8] R. Mukundan, E.L. Brosha, S.A. Birdsell, A.L. Costello, F.H. Garzon, R.S. Willms, Tritium Conductivity and Isotope Effect in Proton-Conducting Perovskites, *J. Electrochem. Soc.* 146 (2019) 2184–2187.
- [9] M.K. Hossain, K. Hashizume, S. Jo, K. Kawaguchi, Y. Hatano, Hydrogen isotope dissolution and release behavior of rare earth oxides, *Fusion Sci. Technol.* 76 (2020) 553–566.
- [10] W. Mao, T. Chikada, A. Suzuki, T. Terai, H. Matsuzaki, Hydrogen isotope dissolution, diffusion, and permeation in  $\text{Er}_2\text{O}_3$ , *J. Power Sources.* 303 (2016) 168–174.
- [11] T. Chikada, T. Tanaka, K. Yuyama, Y. Uemura, S. Sakurada, H. Fujita, X.-C. Li, K. Isobe, T. Hayashi, Y. Oya, Crystallization and deuterium permeation behaviors of yttrium oxide coating prepared by metal organic decomposition, *Nucl. Mater. Energy.* 9 (2016) 529–534.

- [12] Y. Kawamura, K. Isobe, T. Yamanishi, Mass transfer process of hydrogen via ceramic proton conductor membrane of electrochemical hydrogen pump, *Fusion Eng. Des.* 82 (2007) 113–121.
- [13] M.K. Hossain, M.C. Biswas, R.K. Chanda, M.H.K. Rubel, M.I. Khan, K. Hashizume, A review on experimental and theoretical studies of perovskite barium zirconate proton conductors, *Emergent Mater.* (2021).
- [14] M.K. Hossain, K. Hashizume, Y. Hatano, Evaluation of the hydrogen solubility and diffusivity in proton-conducting oxides by converting the PSL values of a tritium imaging plate, *Nucl. Mater. Energy.* 25 (2020) 100875.
- [15] M.K. Hossain, R. Chanda, A. El-Denglawey, T. Emrose, M.T. Rahman, M.C. Biswas, K. Hashizume, Recent progress in barium zirconate proton conductors for electrochemical hydrogen device applications: A review, *Ceram. Int.* 47 (2021) 23725–23748.
- [16] M.K. Hossain, K. Hashizume, Preparation and characterization of yttrium doped barium-zirconates at high temperature sintering, in: *Proceeding Int. Exch. Innov. Conf. Eng. Sci., IGSES, Kyushu University, Fukuoka, Japan, 2019: pp. 70–72.*
- [17] M. Khalid Hossain, K. Hashizume, Dissolution and release behavior of hydrogen isotopes from barium-zirconates, *Proc. Int. Exch. Innov. Conf. Eng. Sci.* 6 (2020) 34–39.
- [18] M.K. Hossain, H. Tamura, K. Hashizume, Visualization of hydrogen isotope distribution in yttrium and cobalt doped barium zirconates, *J. Nucl. Mater.* 538 (2020) 152207.
- [19] M.K. Hossain, T. Iwasa, K. Hashizume, Hydrogen isotope dissolution and release behavior in Y-doped BaCeO<sub>3</sub>, *J. Am. Ceram. Soc.* (2021) jace.18035.
- [20] A.C.T. van Duin, B. V. Merinov, S.S. Han, C.O. Dorso, W.A. Goddard, ReaxFF Reactive Force Field for the Y-Doped BaZrO<sub>3</sub> Proton Conductor with Applications to Diffusion Rates for Multigranular Systems, *J. Phys. Chem. A.* 112 (2008) 11414–11422.
- [21] A. Cammarata, A. Emanuele, D. Duca, Y:BaZrO<sub>3</sub> Perovskite Compounds II: Designing Protonic Conduction by using MD Models, *Chem. – An Asian J.* 7 (2012) 1838–1844.
- [22] K.D. Kreuer, Proton-conducting oxides, *Annu. Rev. Mater. Res.* 33 (2003) 333–359.
- [23] X. Li, L. Zhang, Z. Tang, M. Liu, Fast Oxygen Transport in Bottlelike Channels for Y-Doped BaZrO<sub>3</sub>: A Reactive Molecular Dynamics Investigation, *J. Phys. Chem. C.* 123 (2019) 25611–25617.
- [24] K.-D. Kreuer, S.J. Paddison, E. Spohr, M. Schuster, Transport in Proton Conductors for Fuel-Cell Applications: Simulations, Elementary Reactions, and Phenomenology, *Chem. Rev.* 104 (2004) 4637–4678.
- [25] K. Kurosaki, J. Adachi, T. Maekawa, S. Yamanaka, Thermal conductivity analysis of BaUO<sub>3</sub> and BaZrO<sub>3</sub> by semiempirical molecular dynamics simulation, *J. Alloys Compd.* 407 (2006) 49–52.
- [26] S. Yamanaka, T. Hamaguchi, T. Oyama, T. Matsuda, S. ichi Kobayashi, K. Kurosaki, Heat capacities and thermal conductivities of perovskite type BaZrO<sub>3</sub> and BaCeO<sub>3</sub>, *J. Alloys Compd.* 359 (2003) 1–4.
- [27] W.F. Goh, S.A. Khan, T.L. Yoon, A molecular dynamics study of the thermodynamic properties of barium zirconate, *Model. Simul. Mater. Sci. Eng.* 21 (2013) 045001.
- [28] I. Charrier-Cougoulic, T. Pagnier, G. Lucazeau, Raman Spectroscopy of Perovskite-Type BaCe<sub>x</sub>Zr<sub>1-x</sub>O<sub>3</sub> (0 ≤ x ≤ 1), *J. Solid State Chem.* 142 (1999) 220–227.
- [29] K.T. Jacob, Y. Waseda, Potentiometric determination of the gibbs energies of formation of SrZrO<sub>3</sub> and BaZrO<sub>3</sub>, *Metall. Mater. Trans. B.* 26 (1995) 775–781.
- [30] S. Yamanaka, M. Fujikane, T. Hamaguchi, H. Muta, T. Oyama, T. Matsuda, S. Kobayashi, K. Kurosaki, Thermophysical properties of BaZrO<sub>3</sub> and BaCeO<sub>3</sub>, *J. Alloys Compd.* 359 (2003) 109–113.
- [31] A. Ottochian, G. Dezanneau, C. Gilles, P. Raiteri, C. Knight, J.D. Gale, Influence of isotropic and biaxial strain on proton conduction in Y-doped BaZrO<sub>3</sub>: a reactive molecular dynamics study, *J. Mater. Chem. A.* 2 (2014) 3127.
- [32] N. Kitamura, J. Akola, S. Kohara, K. Fujimoto, Y. Idemoto, Proton Distribution and Dynamics in Y- and Zn-Doped BaZrO<sub>3</sub>, *J. Phys. Chem. C.* 118 (2014) 18846–18852.